U.S. ARMY RDECOM

TECHNICAL REPORT RDMR-WD-12-22

INTEGRATED PRINTED CIRCUIT BOARD (PCB) ACTIVE COOLING WITH PIEZOELECTRIC ACTUATOR

Janice C. Booth and Tracy Hudson
Weapons Development and Integration Directorate
Aviation and Missile Research, Development, and Engineering Center

And

Brian A. English, Michael R.Whitley, and Michael S. Kranz
ENGeniusMicro, LLC
107 Jefferson Street,
Huntsville, AL 35801

September 2012

AMRDEC

DESTRUCTION NOTICE

FOR CLASSIFIED DOCUMENTS, FOLLOW THE PROCEDURES IN DoD 5200.22-M, INDUSTRIAL SECURITY MANUAL, SECTION II-19 OR DoD 5200.1-R, INFORMATION SECURITY PROGRAM REGULATION, CHAPTER IX. FOR UNCLASSIFIED, LIMITED DOCUMENTS, DESTROY BY ANY METHOD THAT WILL PREVENT DISCLOSURE OF CONTENTS OR RECONSTRUCTION OF THE DOCUMENT.

DISCLAIMER

THE FINDINGS IN THIS REPORT ARE NOT TO BE CONSTRUED AS AN OFFICIAL DEPARTMENT OF THE ARMY POSITION UNLESS SO DESIGNATED BY OTHER AUTHORIZED DOCUMENTS.

TRADE NAMES

USE OF TRADE NAMES OR MANUFACTURERS IN THIS REPORT DOES NOT CONSTITUTE AN OFFICIAL ENDORSEMENT OR APPROVAL OF THE USE OF SUCH COMMERCIAL HARDWARE OR SOFTWARE.

REPORT DOCUMENTATION PAGE

Form Approved
OMB No. 074-0188

1. AGENCY USE ONLY	2. REPORT DATE	3. REPORT TYPE AND DATES COVERED
	September 2012	Final

4. TITLE AND SUBTITLE
Integrated Printed Circuit Board (PCB) Active Cooling with Piezoelectric Actuator

5. FUNDING NUMBERS

6. **AUTHOR**(S)
Janice C. Booth, Tracy Hudson, Brian A. English, Michael R. Whitley, and Michael S. Kranz

7. PERFORMING ORGANIZATION NAME(S) AND ADDRESS(ES)
Commander, U.S. Army Research, Development, and Engineering Command
ATTN: RDMR-WDG-R
Redstone Arsenal, AL 35898-5000

8. PERFORMING ORGANIZATION REPORT NUMBER
TR-RDMR-WD-12-22

9. SPONSORING / MONITORING AGENCY NAME(S) AND ADDRESS(ES)

10. SPONSORING / MONITORING AGENCY REPORT NUMBER

11. SUPPLEMENTARY NOTES

12a. DISTRIBUTION / AVAILABILITY STATEMENT
Approved for public release; distribution is unlimited.

12b. DISTRIBUTION CODE
A

13. ABSTRACT ***(Maximum 200 Words)***

Thermal management is challenging in Radio Frequency (RF) communication and radar systems that require high-power levels for operation and reliability as well as small footprints to control intrinsic losses and meet design constraints. An interesting approach uses discrete, in-situ fluid handling and embedded synthetic jet drivers to enhance local cooling at the component. In this approach, fluid cavities and actuators are integrated into the Printed Circuit Board (PCB) near the component. Magnetic and piezoelectric actuators have proven effective in other less demanding applications. The challenge to adapting from magnetic to piezoelectric actuators is to achieve high flow rates because piezoelectric actuators have lower displacement and higher frequencies. This investigation explored frequency and displacement effects on cooling rates for piezoelectric actuators embedded in PCB. Further concept development includes integration with thermal ground planes.

14. SUBJECT TERMS
Printed Circuit Boards (PCB), Radio Frequency (RF), Piezoelectric Actuator

15. NUMBER OF PAGES
21

16. PRICE CODE

17. SECURITY CLASSIFICATION OF REPORT	18. SECURITY CLASSIFICATION OF THIS PAGE	19. SECURITY CLASSIFICATION OF ABSTRACT	20. LIMITATION OF ABSTRACT
UNCLASSIFIED	UNCLASSIFIED	UNCLASSIFIED	SAR

NSN 7540-**01**-280-5500

Standard Form 298 (Rev. 2-89)
Prescribed by ANSI Std. Z39-18
298-102

TABLE OF CONTENTS

LIST OF ILLUSTRATIONS

I. INTRODUCTION

This investigation will evaluate piezoelectric drivers in an active cooling substrate for the targeted thermal management of Radio Frequency (RF) microchips. To control affordability, mature fabrication techniques, common materials, and Commercial Off-The-Shelf (COTS) devices will be investigated. To validate feasibility, active cooling substrates with piezoelectric drivers will be fabricated and tested. A key concern is that reduced displacement and increased frequency of small COTS piezoelectrics will cause a significant reduction in cooling rates. This investigation will benchmark heat removal rates versus frequency and displacement of several piezoelectric disks. From this investigation, an active cooling substrate approach will be demonstrated, and piezoelectric actuator needs will be quantified. This report presents the concept, initial design, fabrication, and experimental setup of this larger investigation.

A lightweight, minimized footprint, air-based thermal solution is ideal for many RF applications. Phased array antennas operating at Millimeter Wave (MMW) frequencies face intense thermal environments that can require heavy, large, liquid-based solutions. These typical thermal solutions can greatly increase the cost and size of the overall system. For small airborne platforms, size, weight, and—with growing budgetary concerns—cost largely prevent the use of phased array technology. Creation of an effective air-based solution could allow for phased arrays to become more prominently featured on platforms where size and weight are important restrictions.

Antenna designs and RF component layouts will have to be adjusted in order to integrate a piezoelectric actuator with cavities and orifices. Phased array antenna elements are normally designed with near half-wavelength spacing between antenna elements. At MMW frequencies, this results in antenna spacing on the order of millimeters. Phased array designs have a heat-producing power amplifier supplying RF energy from one to several antenna elements. This would force the cavities and orifices to be able to be operational in a millimeter to centimeter size gap between heating elements. Additionally, the width of the piezoelectric actuator may encompass several heating elements, forcing a single cooling mechanism to provide the thermal solution to multiple heating elements. This may be mitigated by stacking the cooling mechanisms, but that will impact the overall size of the system.

This concept relies on a cool air source relative to the temperature of the heat element. In many RF environments, the RF components are encapsulated and will not have access to outside air sources. This closed-environment will force the actuators to recycle the same air continuously, resulting in an ever increasing ambient temperature. At some point, the air will no longer be able to cool the active element. Studies will need to be performed to show the length of time it takes to reach the steady-state ambient temperature. It may be necessary to consider a switching technique that allows cool air from another reservoir to be sucked in during the injection phase of the actuator and is then pushed out to the heating element during the ejection phase of the actuator. This would greatly increase the amount of cooling capacity available to the system.

II. CONCEPT

The conceptual device is shown in Figure 1. The cooler substrate is a laminated multilayer FR-4 substrate. Individual layers are patterned to support the active element, form a resonant cavity, and form a flow orifice near the active element. A cavity is machined into the lower levels, and the edges of the cavity support a piezoelectric actuator. The cavity diameter (D_c) is mechanically machined, and the cavity height (H) is controlled by the thickness of the FR-4 layer(s). An exhaust orifice of hydraulic length (h) and hydraulic diameter (D_o) is machined into the middle layers of the Printed Circuit Board (PCB). A top layer finishes the cavity and forms an exhaust port. The cavity and orifice are designed such that the resonance of the working fluid matches the resonance of the piezoelectric membrane. This maximizes displacement and minimizes inertial resistance of the operating fluid. A high-power density active element is placed downstream from the orifice.

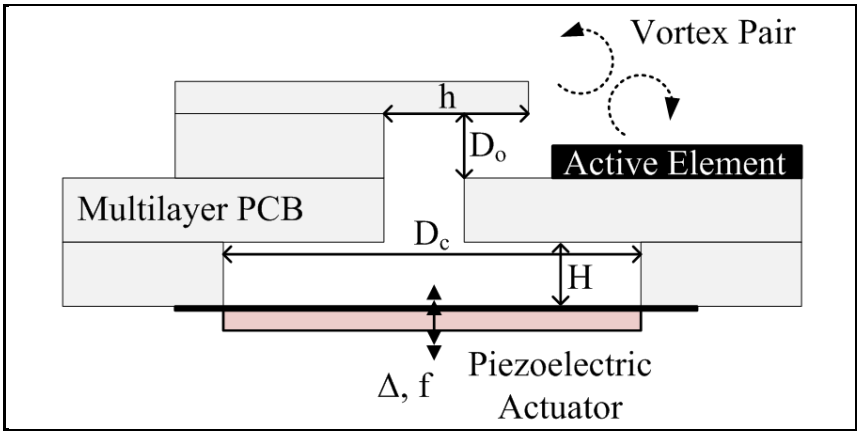

Figure 1. Active Cooling Substrate with Piezoelectric Actuator

During operation, a high voltage amplifier actuates the piezoelectric driver near its mechanical resonant frequency (f), and the displacement (Δ) is controlled by the input voltage. The input affects flow velocity versus time at the exhaust orifice. The oscillation of the flow velocity at the orifice generates vortex pairs that propagate downstream with some velocity. These vortex pairs enhance mixing between ambient air and the thermal boundary layer of the active element [1,2], effectively increasing the amount of heat transferred from the chip to the air and reducing the steady-state chip temperature. This stage of the concept development is focusing on the effects of displacement and frequency on the chip temperature.

III. THEORY OF OPERATION

A. Flow Rates and Chip Location

The voltage and frequency to the piezoelectric membrane controls the amplitude of flow velocity at the orifice exit. The piezoelectric membrane is assumed to be a clamped circular membrane with a load proportional to the input voltage, so it should have a parabolic deflection governed by Equation 1.

$$w(r,t) = -\frac{[q_{max}\cdot \sin(2\pi f t)]}{64\cdot C_1}(a^2 - r^2)^2 \quad (1)$$

where, $$C_1 = \frac{d^3 E}{12 \cdot (1-\lambda^2)} \quad (2)$$

The volume displaced at any time is the integral of this deflection at time (t),

$$V(t) = 2\pi \int_0^a w(r,t) dr = -\frac{\pi\, q_{max} \cdot \sin(2\pi f t)}{60 \cdot C_1} a^5 \quad (3)$$

So, the volumetric flow rate for a given peak deflection is calculated as:

$$\dot{V}(t) = \frac{dV(t)}{dt} = -\frac{\pi^2 \cdot f \cdot q_{max} \cdot \cos(2\pi f t)}{30 \cdot C_1} a^5 \quad (4)$$

At this point, assuming incompressible flow (mass flow rate (Ma) is less than 0.3), the mean flow velocity at the exit orifice is calculated by dividing the volumetric flow rate by the cross-sectional area of the exit. This estimation of flow velocity can then be input into a Finite Element Analysis (FEA) model (as shown in Figure 2) to determine the location of the active element downstream from the flow orifice.

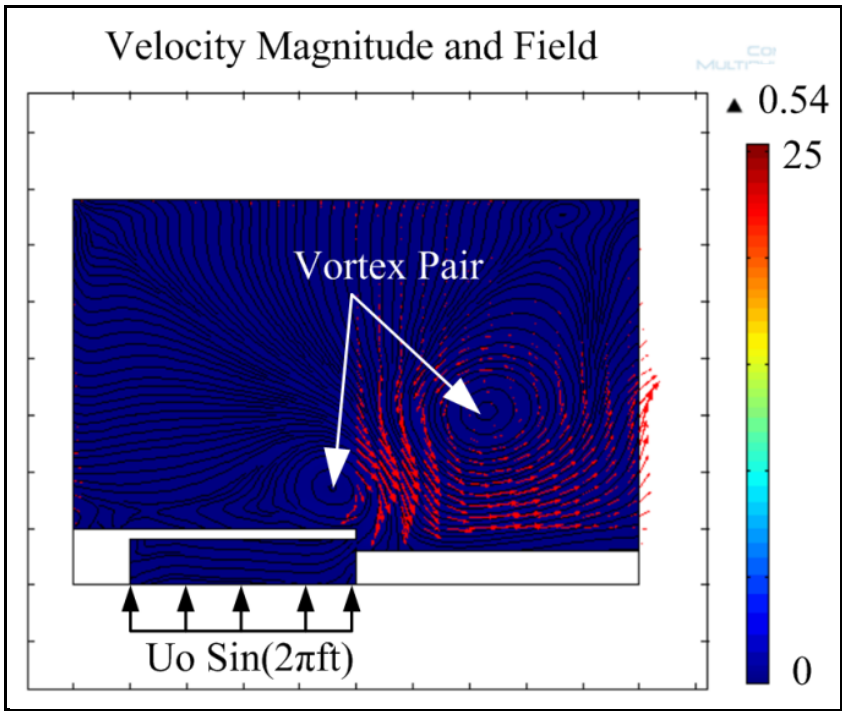

Figure 2. Turbulent Flow Simulation for Sinusoidal Velocity Input at Base of Resonant Cavity

B. Heating Rates

This investigation directly measures thermal effectiveness as a function of input to the piezoelectric driver. During operation, electrical power input to a chip generates waste heat, which increases the temperature of the chip, the substrate, and the surrounding air. The electrical power input into the chip (simply voltage (v) times current (i)) must be stored in the chip and dissipated into the substrate or air. At steady state, the power in equals the power dissipated, and the schematic shown in Figure 3 can be used to approximate heating rates. Increased thermal effectiveness will be evident as increased heat dissipation into the air or increased power input at a given temperature.

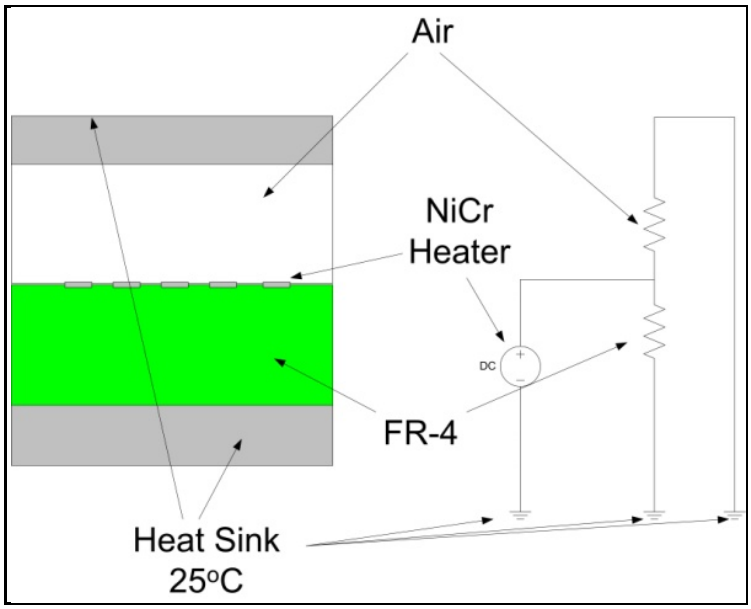

Note: DC Direct Current

Figure 3. Schematic and Electrical Analog of Simulated Active Elements

To quantify heating rates and direction of heat flow, a heater and four Resistive Thermal Devices (RTDs) are added to the conceptual device, as shown in Figure 4. Heat generation from an active RF element is simulated using copper-nickel or nichrome (NiCr) resistors which are fabricated on the surface of a PCB substrate. The heater coil has an area of 0.25 centimeters squared and a power input of 2 watts, for a total heat flux of 8 watts per centimeter squared. Embedded RTDs are added to the conceptual device to facilitate these heating measurements, as shown in Figure 4. The device includes two embedded RTDs below the active element, one RTD at the exhaust orifice, and one RTD in the main resonant cavity. The two RTDs embedded in the PCB (T_1 and T_2) measure heat flow into the PCB itself. The third RTD (T_3) detects heated air drawn into the cavity, and the fourth RTD (T_4) measures the bulk cavity temperature. In addition, T_4 determines the actual resonant frequency of the cavity for air, as determined by the following Equation 5 [3]:

$$f_H = \frac{1}{2\pi}\sqrt{\frac{c(T)^2 \cdot D_o^2}{\gamma(T) \cdot H \cdot h \cdot D_c^2} - \frac{256 \cdot \upsilon(T)^2}{D_o^4}} \tag{5}$$

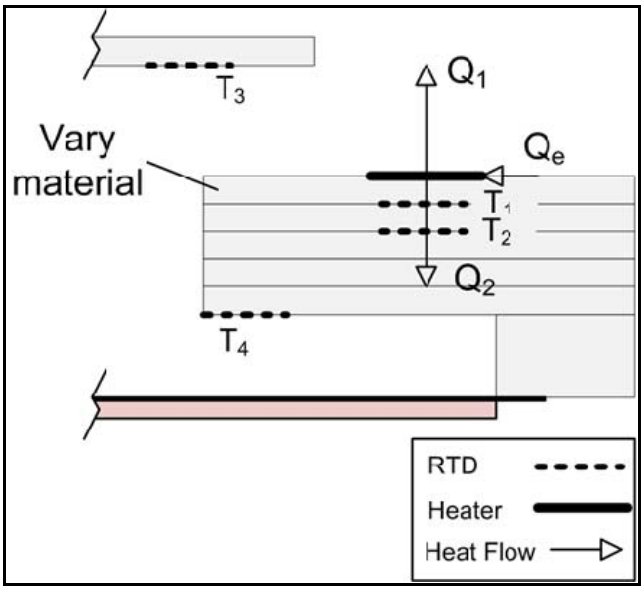

Figure 4. Conceptual RTD Placement for Heat Flow Measurements

IV. FABRICATION

A. Fabrication

Device fabrication follows standard PCB processing. Initial devices were fabricated using multilayer FR-4 boards and prepreg epoxy. Individual FR-4 lamina were mechanically machined to pattern each layer. The layers were aligned, stacked, and laminated to form the Three-Dimensional (3-D) device. Typically, PCB interlayers have 34 μm thick copper cladding. As an alternative to this material, devices were laminated with 70/30 copper-nickel alloy or 80/20 nickel-chrome alloy and patterned by means of photolithographic techniques and wet etching in a ferric chloride bath.

The fabricated layers (as shown in Figure 5) consisted of a substrate, an experimental layer, an orifice layer, and a cap layer. The base layer contained a hole which centered the piezoelectric driver. The experimental layer contained a shoulder to set the resonant cavity height, two RTDs to determine heat flux into the board, and a copper-nickel heater to simulate a thermal source. The orifice layer formed the flow orifice and set the downstream distance to the heater. The cap layer sealed the resonant cavity and contained an RTD at the orifice and in the center of the cavity.

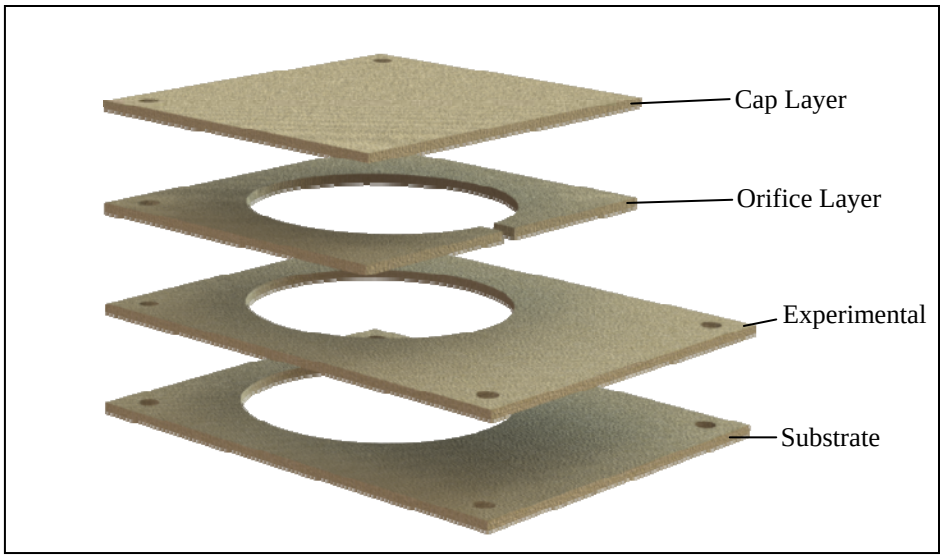

Figure 5. Multilayer PCB Fabrication

B. Fabrication Results

Fabrication results are shown in Figure 6. In the top left photo, the cap layer is removed to show the resonant chamber and the flow orifice. In the top right photo, the cap layer is bonded, and the total board dimensions are 40-by-25 millimeters.

Figure 6. Fabricated 9-Kilohertz Active Cooler Board

After boards are laminated, a piezoelectric membrane (Figure 7) and a heater (Figure 8) are installed.

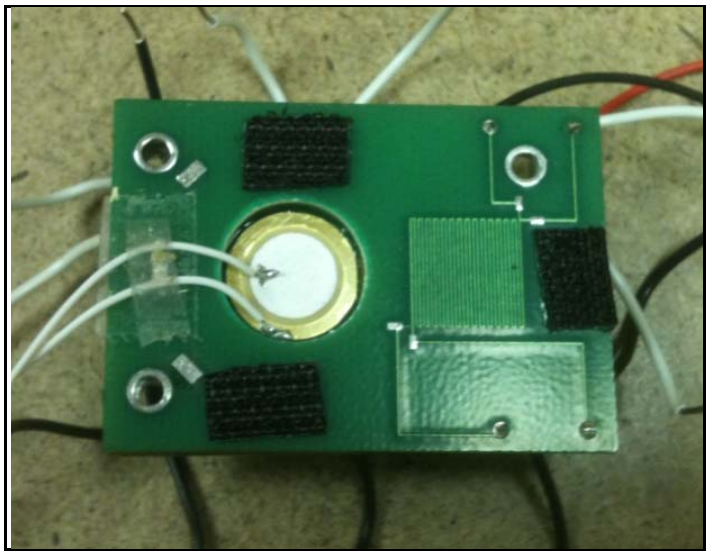

Figure 7. Substrate Board with Piezoelectric Element Installed and Lower RTD

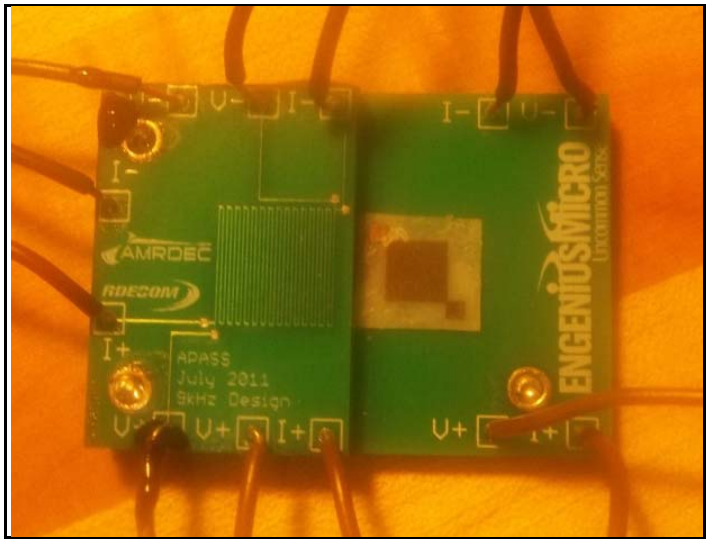

Figure 8. Experimental Board with Heater Element

V. EXPERIMENTAL SETUP

The test bed consists of National Instruments Data Acquisition (DAQ) hardware (USB-6259), a copper-nickel heating element, signal conditioning electronics, and the unit under test. A based Personal Computer (PC) is used to interface with the DAQ hardware and control the test.

To control the heater, a Pulse Width Modulated (PWM) signal (generated by the DAQ board) controls a constant current source to a transistor between the current source and the heating element. Varying the duty cycle of the PWM signal controls the effective heating rate of the heater elements. The heater element functions as an RTD as well as a heater. The heater voltage for a given input current determines the heater temperature. Electronics condition the heater voltage for a readout by the DAQ system.

The control circuit for the heater is shown in Figure 9, and the characterization of the heater control is shown in Figure 10.

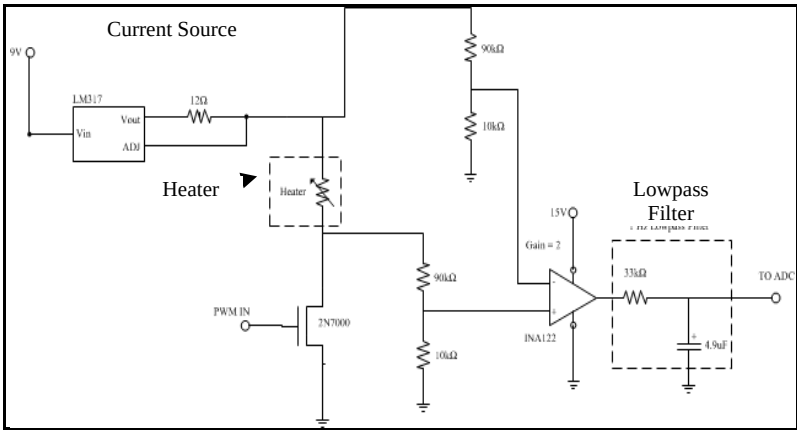

Figure 9. Heater Control Schematic

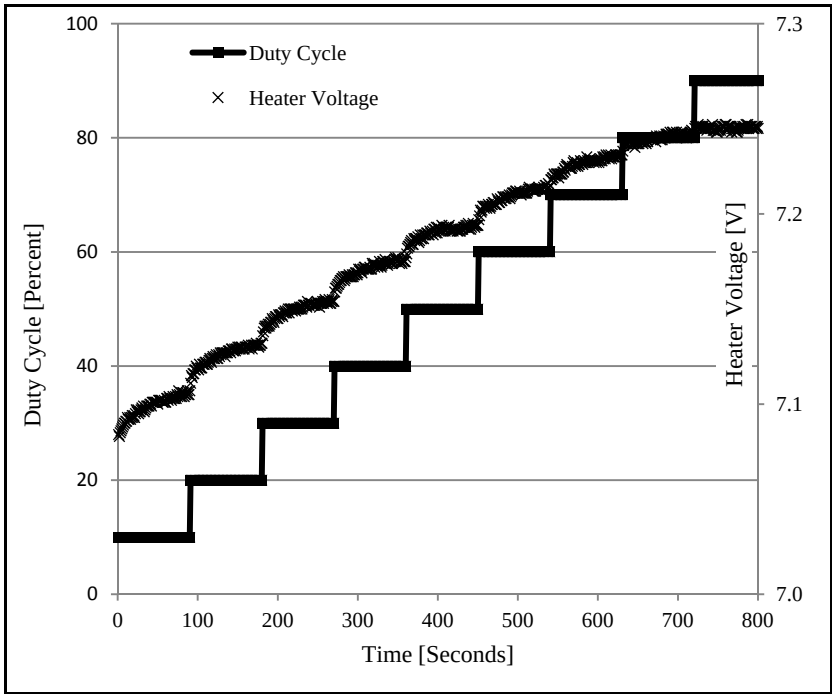

Figure 10. Heater Characterization Versus Pulse Width Duty Cycle

There are three RTDs embedded in the unit under test. To make a measurement, constant current is applied to the RTD and voltage is measured. The RTDs were made with a standard PCB manufacturing process, so the temperature sensitivity is very small. A voltage amplifier and offset removal are used to achieve a more accurate voltage measurement and thus an accurate measure of the RTD temperature.

The C#.NET, with the National Instruments DAQmx drivers, is used to interface with the DAQ control system to develop a control system. The control system (as shown in Figure 11) reads each RTD temperature independently, applies a driving signal to the heater and the piezoelectric element, reads the heater temperature, and plots all pertinent data.

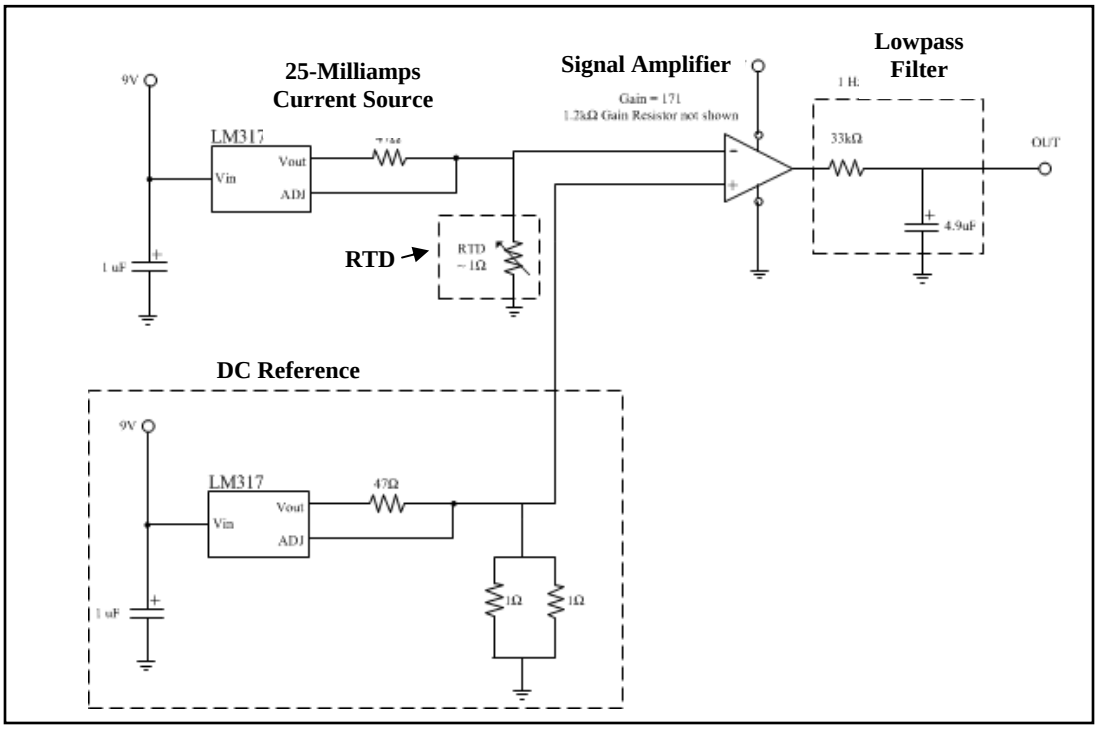

Note: Vin=Voltage In, Vout= Voltage Out

Figure 11. RTD DAQ Schematic

VI. RESULTS

This report has provided results on three key points to date. Affordable fabrication and experimental setup were shown in the previous two sections. In the final result, piezoelectric actuation voltage and frequency were shown to decrease chip temperature and increase heat transfer to the substrate using the hardware and process described.

Figure 12 shows temperature data for the heater and RTDs versus frequency to the piezoelectric driver. In this case, the piezoelectric was driven at 10 volts between 0 to 1 kilohertz. The PWM controller to the heater was held at a constant 99 percent. This board was designed to resonate at 600 hertz. There was an audible increase in sound volume around 400 hertz, which corresponded to a dip in heater temperature. This is attributed to Helmholtz resonance of the cavity.

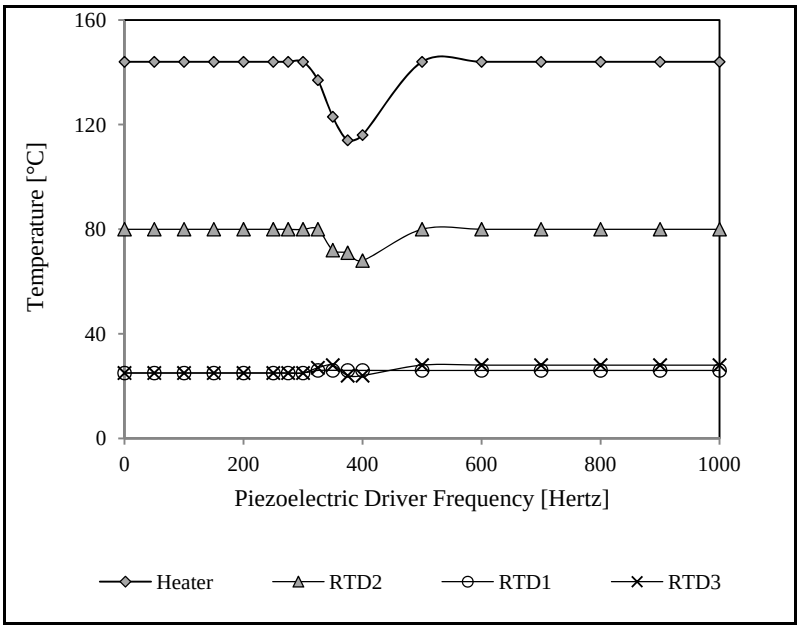

Figure 12. Active Cooling Board Temperature Profiles Versus Piezoelectric Drive Frequency

The effect of piezoelectric drive voltage and frequency on heater temperature is shown in Figure 13. The piezoelectric drive frequency was increased by 20 hertz every 10 seconds, and the piezoelectric drive voltage was varied between 4 and 10 volts. Increasing the drive voltage to the piezoelectric increased the displacement and flow rate from the orifice. As a result, the heater temperature decreased with increased flow rate and drive voltage. Again, evidence of Helmholtz resonance was observed between 400 to 420 hertz.

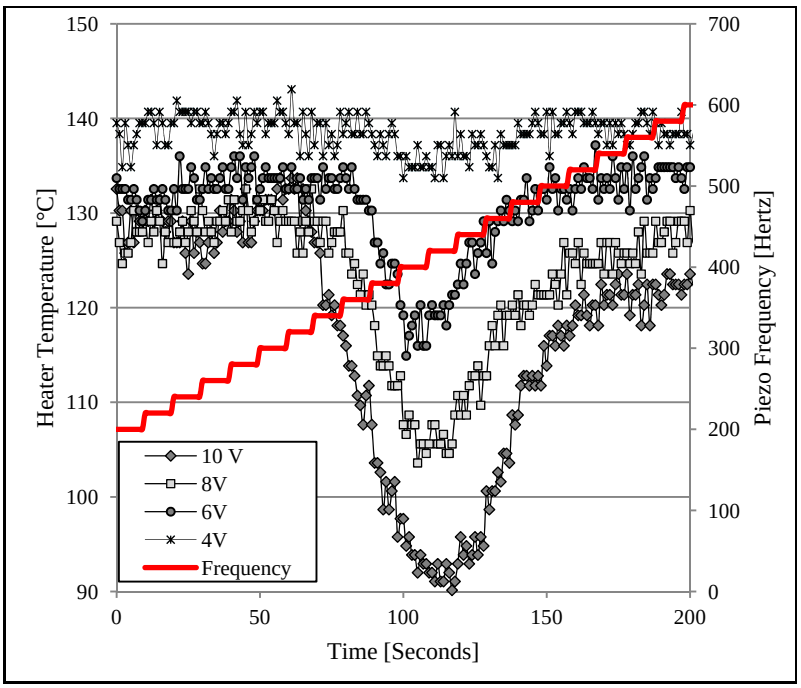

Figure 13. Piezoelectric Drive Voltage and Frequency Effects on Heater Temperature

Finally, heat transfer into the board was calculated based on the heater temperature and RTD. The heater and RTD are separated by 1.56 millimeters of FR-4, and heat transfer to the board was calculated for One-Dimension (1-D) conduction. The heater area was 0.25 centimeters squared so that the heat flux into the board could be calculated by dividing by this number. As with the heater temperature, the heat transfer was shown to be more effective at resonance with a higher piezoelectric drive voltage, as shown in Figure 14.

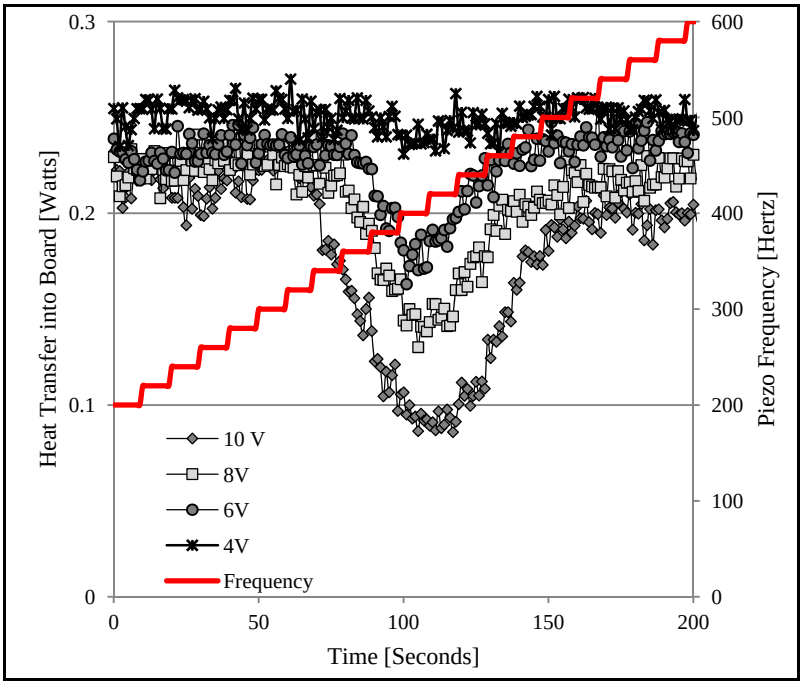

Figure 14. Piezoelectric Drive Voltage and Frequency Effects on Heat Transfer to Board

The chip consumed 0.378 watts per centimeters squared of electric power and a steady-state temperature of 70 °C. With piezoelectric actuation, testing showed a temperature reduction to 51 °C. The overall thermal resistance, including both PCB and air, decreased 34 percent from 208 to 138 Kelvin per watts. If the base temperature of the board is held constant, this equals a 91-percent reduction in thermal resistance to the air, from 3,333 to 365 Kelvin per watts. These results show a change in heat transfer coefficient from 12 watts per meters squared Kelvin without piezoelectric actuation to 110 watts per meters squared Kelvin with piezoelectric actuation. These numbers are in line with typical natural and forced convection numbers, respectively. Further results are needed to compare piezoelectric input parameters and PCB design parameters to total cooling rates.

VII. CONCLUSIONS

Three key points have been demonstrated in this report. First, an affordable fabrication plan to adapt the magnetic-actuated active cooling substrate to a piezoelectric-actuated active cooling substrate has been demonstrated. Second, an experimental setup has been developed and implemented for validating the cooling rates of this concept. Finally, the piezoelectric-actuated active cooling substrate was demonstrated to decrease the temperature of a single chip.

There are a number of issues to be resolved going forward. First, fabrication is fairly straightforward without thermal ground planes and COTS actuators. Additional work will be needed to include high-thermal conductivity materials, high-temperature substrates, and a reduced overall size. The lamination approach is still viable with these material changes, but processing conditions will require validation as size scales are reduced and various materials are integrated into the process.

Second, experiments clearly showed that cavity resonance and increased piezoelectric drive voltages improve cooling rates and better reduce heater temperature. However, there was no indication of another dip when the piezoelectric actuator was in mechanical resonance. Further validation is needed to confirm the efficacy of the piezoelectric actuation for active cooling substrates as a function of input parameters—drive voltage, frequency, and downstream distance. The magnetic-actuation reference [2] and previous piezoelectric references [4,5] suggest that target actuation rates should be in the 100-hertz range with large flow rates. If these conditions are required for the piezoelectric-actuated active cooling substrate, then one challenge going forward will be to develop high-displacement piezoelectric actuators within the fabrication process. In addition to the straightforward simple case of this investigation, the option to cool multiple chips with a single driver is also available.

IIX. SUMMARY

A fabrication approach, experimental setup, and completed preliminary testing of a piezoelectric-actuated active cooling substrate have been developed. Discrete, in-situ fluid handling and embedded synthetic jet drivers were used to enhance local cooling at a heated component. The fluid cavities and actuators were integrated into the PCB near the component. Frequency and displacement effects on cooling rates for piezoelectric actuators embedded in PCB have been explored.

REFERENCES

1. Gillespie, M.B. et al., "Local Convective Heat Transfer From a Constant Heat Flux Flat Plate Cooled by Synthetic Air Jets,"ASME Journal of Heat Transfer, Volume 128, pp. 990-1000. October 2006.

2. Wang, Young et al., "Active Cooling Substrates for Thermal Management of Microelectronic," IEEE Transactions on Components and Packaging Technology, Volume 28, pp. 477-83, September 2005.

3. Tang, H. and Zhong, S., "A Static Compressible Flow Model of Synthetic Jet Actuators," The Aeronautical Journal, pp. 421-31, July 2007.

4. Mahalingam, Raghav; Rumigny, Nicolas; and Glezer, Ari, "Thermal Management Using Synthetic Jets," IEEE Transactons on Components and Packaging Technologies, Volume 27, pp. 439-44, 2004.

5. Glezer, Ari et al., "Synthetic Jet Actuators and Applications Thereof," Patent Number 5,758,823, June 1998.

LIST OF ACRONYMS AND ABBREVIATIONS

1-D	One-Dimensional
3-D	Three-Dimensional
COTS	Commercial Off-The-Shelf
DAQ	Data Acquisition
DC	Direct Current
D_c	Cavity Diameter
D_o	Hydraulic Diameter
FEA	Finite Element Analysis
H	Cavity Height
h	Hydraulic Length
Ma	Mass Flow Rate
MMW	Millimeter Wave
NiCr	Nichrome
PC	Personal Computer
PCB	Printed Circuit Board
PWM	Pulse Width Modulated/Modulation
RF	Radio Frequency
RTD	Resistive Thermal Device
Vin	Voltage In
Vout	Voltage Out
µm	micrometer

INITIAL DISTRIBUTION LIST

		Copies
Weapon Systems Technology Information Analysis Center Alion Science and Technology 201 Mill Street Rome, NY 13440	Ms. Gina Nash gnash@alionscience.com	Electronic
Defense Technical Information Center 8725 John J. Kingman Rd., Suite 0944 Fort Belvoir, VA 22060-6218	Mr. Jack L. Rike jrike@dtic.mil	Electronic
AMSAM-L	Ms. Anne C. Lanteigne anne.lanteigne@us.army.mil	Electronic
	Mr. Michael K. Gray michael.k.gray@us.army.mil	Electronic
RDMR	Mr. Steve Cornelius steve.cornelius@us.army.mil	Electronic
RDMR-CSI		Electronic
RDMR-WD	Dr. Robin Buckelew robin.buckelew@us.army.mil	Electronic
	Mr. Jim Hatfield jim.hatfield@us.army.mil	Electronic
RDMR-WDG-C	Dr. Roger Berry roger.berry@us.army.mil	Electronic
RDMR-WDG-R	Ms. Janice C. Booth janice.c.booth@us.army.mil	Electronic
	Mr. Joel P. Booth joel.booth@us.army.mil	Electronic
	Mr. Chris Hamner chris.hamner@us.army.mil	Electronic
	Mr. Randy McElroy randy.mcelroy@us.army.mil	Electronic
	Mr. Jim Mullins jim.mullins@us.army.mil	Electronic
	Dr. Brian Smith brian.smith@us.army.mil	Electronic
RDMR-WDR	Dr. Paul Ruffin paul.ruffin@us.army.mil	Electronic

INITIAL DISTRIBUTION LIST (CONCLUDED)

		Copies
RDMR-WDR-S	Dr. Jim Baumann jim.baumann@us.army.mil	Electronic
	Mr. Heinz Sage heinz.sage@us.army.mil	Electronic
	Ms. Loretta Painter loretta.painter@us.army.mil	Electronic
ENGeniusMicro, LLC 107 Jefferson Street Huntsville, AL 35801	Mr. Brian A. English brain.english@engeniusmicro.com	Electronic
	Mr. Michael R. Whitley michael.whitley@engeniusmicro.com	Electronic
	Mr. Michael S. Kranz michael.kranz@engeniusmicro.com	Electronic